Effects of Polymeric Motion on ^{19}F NMR Multiple Quantum Coherences: Signal Refocusing in Poly(tetrafluoroethylene)

David A. Lathrop and Karen K. Gleason*

Department of Chemical Engineering, Massachusetts Institute of Technology, Cambridge, Massachusetts 02139

Received December 31, 1992; Revised Manuscript Received June 7, 1993

ABSTRACT: We report a new technique for probing polymer dynamics through the refocusing of multiple quantum (MQ) nuclear magnetic resonance (NMR) coherences. The MQ-NMR experiment follows the correlated behavior of multiple spin-$^1/_2$ nuclei interacting through dipolar couplings. Motion which modulates the dipolar coupling strengths on the same time scale as the experiment alters the intensity of the observed coherences. Temperature-dependent data are presented on poly(tetrafluoroethylene) samples of varying crystallinity. The MQ refocusing experiment is able to clearly differentiate between polymer samples which have different thermal histories. The transitional features observed are discussed in terms of the signatures of various types of molecular level motion.

Introduction

Multiple quantum nuclear magnetic resonance (MQ-NMR) experiments in solids[1] have been successfully applied to problems of proton distributions in amorphous silicon,[2] silicon carbide,[3] and synthetic diamond[4] and adsorption of organic molecules in zeolites[5] and on catalytic surfaces.[6] ^{19}F MQ-NMR has been used to elucidate fluorine distributions in salts[7] and photosensitive polymer mixtures.[8] While previous studies have concerned the atomic distribution in samples that are rigid, in this study we hope to show the usefulness of using MQ-NMR to study molecular motions in polymers. To this end we have used the traditional method of analysis of MQ-NMR data as well as a new type of analysis involving the temperature-dependent behavior of the MQ coherence refocusing.

Background

MQ-NMR. The basic MQ-NMR experiment used is illustrated schematically in Figure 1. The experiment can be divided into separate preparation, mixing, and detection periods. The eight-pulse cycle used during the preparation period is shown at the bottom of Figure 1. A similar eight-pulse sequence, in which each x or $-x$ pulse is replaced by a y or $-y$ pulse, is used during the mixing period. The preparation period is designed to build up even-order coherences, which are then refocused to an observable signal during the mixing period in a process referred to as time reversal.[9] To resolve the various MQ orders, the phases of the pulses used during the mixing period are varied with respect to the phases of the preparation period pulses.[10] The size of the spin system is normally then inferred from the distribution of intensities among the various MQ orders by assuming that n-quantum intensities are proportional to $\exp(-n^2/N_e(\tau))$, with $N_e(\tau)$ being a time-dependent effective spin cluster size.[11]

To understand the effects of molecular motion on MQ-NMR experiments, we must understand the role of the internuclear dipolar coupling constants on the development and refocusing of the multiple quantum coherences. Traditional analysis of the MQ-NMR experimental results has been based on average Hamiltonian theory, which describes the evolution of the spin system under the effect of the MQ pulse sequence.[13] This calculation considers the internal Hamiltonian describing the homonuclear dipolar interactions in the sample to be time independent. If the dipolar couplings in a solid have a constant value on the NMR time scale, the average Hamiltonian H_{yx} is

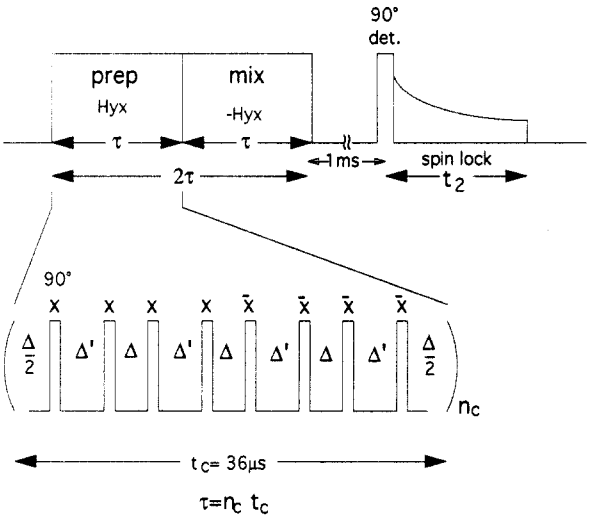

Figure 1. Basic outline of the MQ-NMR experiment with pulse sequence used in preparation period. Pulses in sequence are all 90° pulses. The mixing period pulse sequence is identical to the preparation period sequence, except for the substitution of y and $-y$ pulses for the x and $-x$ pulses shown to achieve time reversal.

created during the preparation period:

$$H_{yx} = -\frac{1}{2}\sum_{j<k} D_{jk}(I_{+j}I_{+k} + I_{-j}I_{-k}) \qquad (1)$$

$I_{\pm j}$ and $I_{\pm k}$ are the quantum mechanical raising and lowering operators. The form of H_{yx} shows that only even-order coherences are created. D_{jk} is the dipolar coupling constant for each pair of interacting nuclei j and k and can be written as

$$D_{jk} = \frac{\gamma^2\hbar}{2r_{jk}^3}(1 - 3\cos^2\chi_{jk}) \qquad (2)$$

γ is the gyromagnetic ratio for the relevant nuclei, $\hbar$ is Planck's constant divided by 2π, r_{jk} is the internuclear distance, and χ_{jk} is the angle between the vector $\mathbf{r}_{jk}$ and the external magnetic field $\mathbf{B}_0$. Thus, any motion which varies either r_{jk} or χ_{jk} will affect the Hamiltonian H_{yx}.

In rigid systems, the dipolar coupling constants upon which the Hamiltonians depend are equal during the preparation and mixing periods. Thus, in the absence of molecular motion, relaxation effects, and phase incrementation, the Hamiltonian $-H_{yx}$ is created during the mixing period, and the spin system at the end of the mixing

0024-9297/93/2226-4652$04.00/0

period can be described by the density matrix $\rho(2\tau)$, which evolves according to the Liouville equation:

$$\rho(2\tau) = \exp(-iH_{yx}\tau)\exp(iH_{yx}\tau)\rho(0)\exp(-iH_{yx}\tau)\times \exp(iH_{yx}\tau) = \rho(0) \quad (3)$$

Equation 3 shows that when the Hamiltonians representing the preparation and mixing periods are equal in magnitude but opposite in sign, the corresponding propagators form a complex conjugate pair, and thus $\rho(2\tau) = \rho(0)$. This result means the state of the spin system, and thus the signal intensity after the detection pulse, should be identical to the initial state irrespective of 2τ. This condition is referred to as time reversal[9,15] and in the absence of relaxation should result in all of the magnetization being refocused at the end of the mixing period.

Motion at frequencies much higher than the MQ time scale (typically 1–10 kHz) results in an averaging of the dipolar coupling strengths. We can consider these cases in terms of the static theory in which we use the averaged couplings to describe the coherence development. This has been seen in previous MQ-NMR experiments using liquid crystal solvents,[14] plastic crystals such as adamantane,[4,15] and salts containing AsF_6^- ions.[7,8] In general, rapid motion causes a decoupling of the spin system which results in a slowing of the development of MQ coherences.

In this paper, we examine the behavior of MQ coherence refocusing when variations of the dipolar coupling constants occur as a result of molecular motion on the time scale of the experiment. Clearly, random variations of the internuclear vectors over the course of the experiment should not result in time reversal. We use the intensity of the refocused signal as a measure of the effectiveness of time reversal. This, in general, should be adversely affected by molecular motion.

Poly(tetrafluoroethylene). Poly(tetrafluoroethylene) (PTFE) is a partially crystalline polymer which has been extensively studied using X-ray diffraction,[16,17] differential scanning calorimetry (DSC),[18] nuclear magnetic resonance (NMR),[19–21] mechanical relaxation,[22,23] and dielectric loss[24] techniques. PTFE undergoes two first-order crystalline transitions at 292 and 303 K as well as three viscoelastic relaxations termed α, β, and γ.[25] The γ-relaxation occurs at ca. 160 K in the amorphous chains and is believed to consist of torsional motions of polymeric backbone segments.[26] The activation energy of the γ-relaxation has been determined to be about 18 kcal/mol.[19] Upon further increase in temperature to 292 K, PTFE undergoes the first of two first-order crystalline transitions. This first transition corresponds to a slight uncoiling of the crystalline helix from 13 carbon atoms per 180° twist to 15 carbon atoms per 180° twist. The unit cell is triclinic below 292 K and hexagonal above 292 K. Between 292 and 303 K, small-angle oscillations of chain segments about a preferred crystallographic direction are believed to occur.[17]

The second first-order crystalline transition is seen at 303 K and involves a further uncoiling of the molecules in the crystalline phase. Above 303 K the oscillation of the molecular segments occurs with a random angular orientation in the lattice, and the preferred crystallographic direction is lost.[17] Translational displacement of molecules in the crystalline region along the chain axis is believed to begin after this second transition.[20] The α-relaxation occurs above 400 K and involves both amorphous and crystalline regions. PTFE finally melts at ca. 600 K.

The β-relaxation overlaps with the two phase transitions and is commonly associated with torsional oscillations and rotations of chain segments around the chain axes in the crystalline regions. The decrease in the NMR line width over this temperature range seen by various authors[19] indicates that the chain rotations begin well below the crystalline transitions, at ca 250 K. The motions associated with the β-relaxation are still, however, linked to the uncoiling of the helix that occurs during the phase transitions.[20]

In virgin samples of as-polymerized PTFE there is evidence of the presence of two crystalline phases. Differential thermal analysis (DTA) has shown double peaks for the crystalline transitions in as-polymerized PTFE, and a viscoelastic anomaly has been observed in samples of virgin PTFE at ca. 208 K that is not seen in melt-crystallized samples.[22] Likewise, Vega and English[20] have seen two component $T_{1\rho}$ and T_{1xz}^{REV} decays in virgin PTFE, which suggests the presence of two crystalline phases with differing mobilities. They also found that the percentage of signal that relaxes with a short T_{1xz}^{REV} increases from <20% at 243 K to almost 70% at 293 K. This indicates that the virgin polymer contains more than one crystalline-like phase, with the higher mobility fraction growing as the temperature increases.[20] The motion responsible for the 208 K viscoelastic anomaly in the more mobile crystalline phase is not well understood, but it has been attributed to segmental motions in paracrystalline regions that contain mobile conformational defects[28] and irregular interchain spacings.[23]

Experimental Section

The MQ-NMR experiments were performed on a home-built NMR spectrometer operating at 270 MHz. Phase incrementation of the preparation period pulses with respect to the mixing period pulses was achieved with a 240-MHz Sciteq digital synthesizer with 8-bit phase resolution. The incremental preparation phase shift was set at 5.6°, allowing detection of coherences with $|n| \leq 16$.

The length of the $\pi/2$ pulses used ranged from 1.6 to 2.0 μs. The basic MQ pulse sequence time was held fixed at 36 μs (40 μs in later runs). A pulsed spin-locking sequence of 5 ms in length containing 500 windows was used during the detection period for signal enhancement.[8] The signal intensity experiments were performed at a phase shift of 90° (time reversal) and long relaxation delays ($>5T_1$) for maximum signal strength. Note that the spin lock sequence is used only to improve the signal to noise ratio of the detected magnetization and does not play a role in the refocusing of the coherences.

The MQ intensity experiments were performed on DuPont dispersion polymerized T-60 in its as-polymerized form as well as after melting and slow cooling. The weight percent crystallinities of these two samples, as calculated from their densities, were determined to be 98% and 64%, respectively.

Results and Discussion

Shown in Figure 2 are the $N_e(\tau)$ values obtained on an as-polymerized PTFE sample as a function of temperature for $\tau = 108$ μs. Below the 292 K transition, the effective number of correlated ^{19}F spins, $N_e(108\ \mu s)$, is 16 ± 2. A sharp decrease in $N_e(\tau)$ begins just before the first crystalline transition and ends near the second crystalline transition. This is the same temperature range over which a sharp decrease in the NMR line width is seen in PTFE.[19] We thus attribute the decrease in effective cluster size with increasing temperature to slower MQ coherence growth due to the decrease of motionally averaged dipolar couplings as well as to the preferential destruction of the refocusing of high-order coherences through molecular motion.

Above the second crystalline transition at 303 K, the values of $N_e(\tau)$ begin to stabilize at about 5 or 6. As pointed out earlier, incoherent rotation and translational slippage of the chains begin to occur above the 303 K transition.

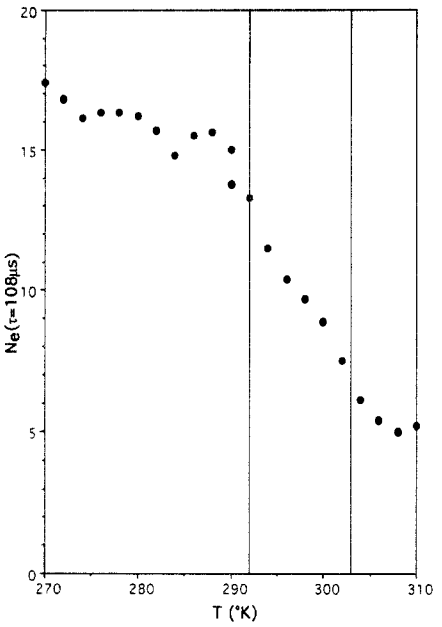

Figure 2. Effective spin cluster size, $N_e(\tau)$, as a function of temperature for τ = 108 μs in as-polymerized poly(tetrafluoroethylene). The vertical lines represent the two first-order crystalline transitions seen at 292 and 303 K in PTFE. The decrease in $N_e(\tau)$ with increasing temperature is attributed to molecular motion in the sample.

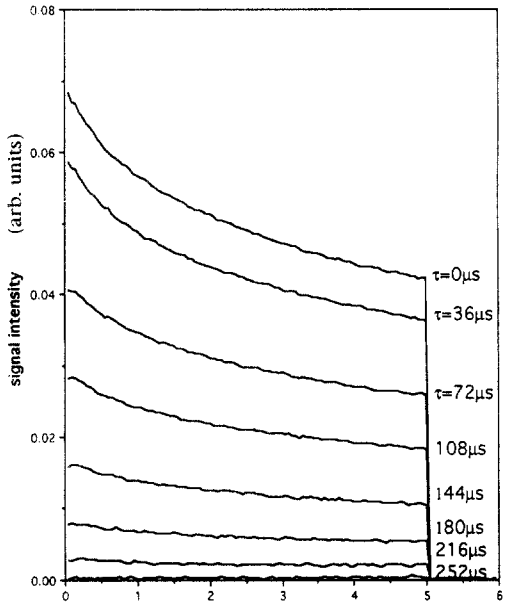

Figure 3. Detected signal for seven different MQ experiments with increasing τ under a spin lock sequence of 5-ms duration. Each experiment differs only in the integral number of the basic 36-μs pulse sequence (n_c = 0, 1, 2, ..., 7) performed in both the preparation and mixing cycles. The topmost signal is from the experiment utilizing only a detectable pulse and is used a standard for comparison.

These motions should quickly destroy the refocusing of any MQ coherences involving interchain fluorines, leaving only MQ coherences involving intrachain couplings to figure into the analysis and calculation of $N_e(\tau)$. The intrachain couplings should not be very dependent on the rate of chain slippage, thus explaining the relatively constant values of $N_e(\tau)$ obtained above 303 K. The $N_e(\tau)$ values at this point should then represent only that coherence growth occurring along the axes of the rotating chains.

Shown in Figure 3 is a representative set of MQ is signal intensity data. The uppermost line represents the signal intensity in the spin lock windows following a single 90° pulse when no MQ excitation is employed. The lines below represent the signal intensities under the identical spin lock sequence when an integral number (n_c) of the 36-μs, eight-pulse preparation and mixing cycles have been performed prior to the 90° detection pulse ($\tau = n_c t_c$, where t_c = 36 μs and n_c = 1, 2, 3, ..., 7).

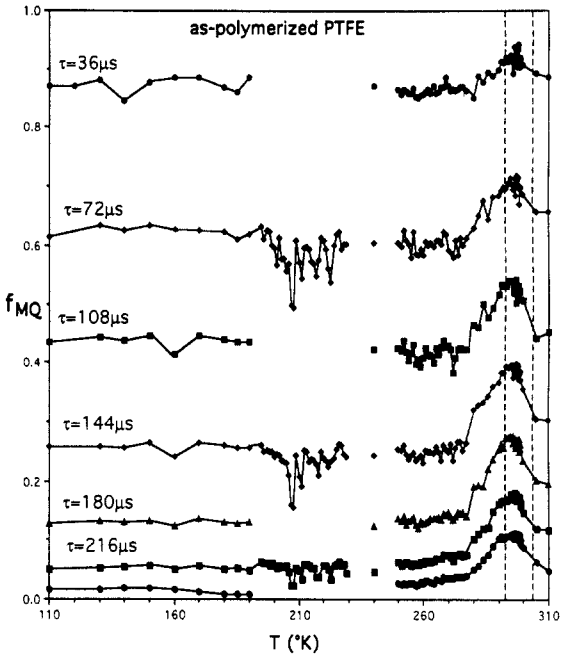

Figure 4. Fractional signal intensity, f_{MQ}, as a function of temperature for seven preparation times, τ, in as-polymerized PTFE.

The signal intensity in the spin lock MQ detection period $S(t_2,\tau,T)$ was divided by the corresponding intensity for the pure spin lock experiment, $S(t_2,0,T)$. We call this ratio f_{MQ}, and it represents the fractional magnetization remaining after the MQ preparation and mixing periods. By using a ratio, temperature-dependent variations in probe tuning or differences in the Boltzmann population of the spin-$^1/_2$ eigenstates should be eliminated. We have found f_{MQ} to be nearly independent of t_2 at a given evolution time τ and temperature T. This allows us to average the f_{MQ} ratios over a range of t_2 values to achieve an increase in the signal to noise ratio.

Shown in Figure 4 are the values of $f_{MQ}(\tau,T)$ thus obtained for the 98% crystalline as-polymerized PTFE sample. Figure 5 shows the values of $f_{MQ}(\tau,T)$ likewise obtained for the 64% crystalline melted chip PTFE sample. For the sake of the following discussion, the same data are replotted for three temperature subranges in Figures 6–8.

In Figure 6 are shown that f_{MQ} values obtained for the melt-crystallized samples from 120 to 230 K. For comparison, the data for the as-polymerized PTFE are shown up to 200 K. The melt-crystallized sample shows higher f_{MQ} values than the as-polymerized sample at the lowest temperatures. If we assume that at these temperatures all regions are static, then some other factor causes the melt-crystallized sample to have a slower loss of signal intensity than the more highly crystalline as-polymerized sample. While we do not understand what process is responsible for the loss of MQ signal intensity in static samples, we can note that its behavior bears some resemblance to the process of spin diffusion.

Spin diffusion is a zero-quantum "flip-flop" process by which local magnetization can equilibrate. The rate of spin diffusion has been shown to be slower in an amorphous region than in a corresponding crystalline region. This is

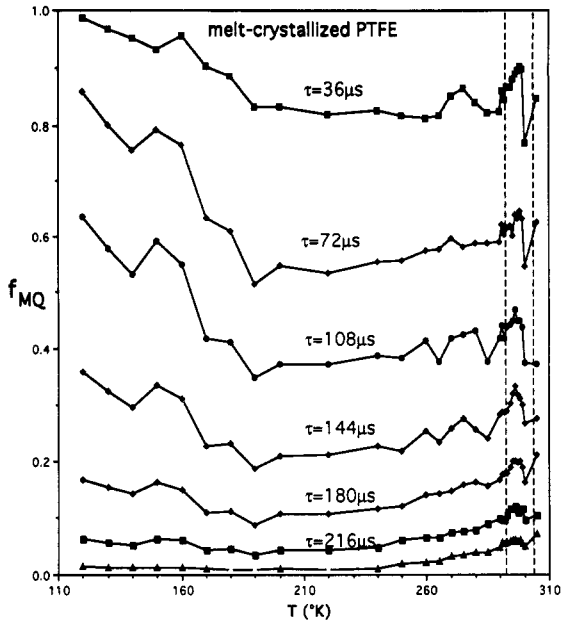

Figure 5. Fractional signal intensity, f_{MQ}, as a function of temperature for seven preparation times, τ, in 64% crystalline, melt-crystallized PTFE.

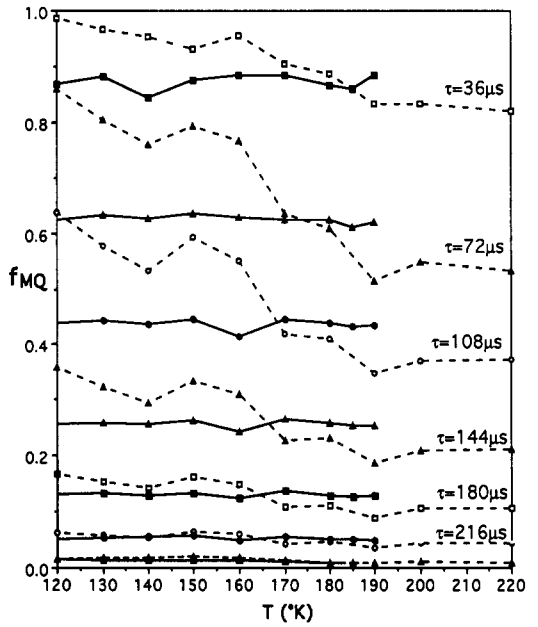

Figure 6. Fractional signal intensity, f_{MQ}, in 64% crystalline, melt-crystallized (open symbols, dotted lines) and as-polymerized (solid symbols, solid lines) PTFE from 120 to 220 K. The overall decrease in the f_{MQ} values in the melt-crystallized sample between 150 and 200 K is attributed to random motions in the amorphous region.

because the mutual spin flips, which are the source of spin diffusion, must be energy conserving. The structural disorder present in amorphous materials causes a wider chemical shift and orientational dispersion, which decreases the probability of a good energy match between adjacent spins and thus slows the spin diffusion rate.[12] The rate of spin diffusion in solids also depends on the average dipolar coupling strength. In other words, magnetization will diffuse faster in a more strongly coupled spin network than in a more weakly coupled network. If a process similar to zero-quantum spin diffusion is responsible for the relaxation of our MQ signal in static systems, then this would account for the slower decay of f_{MQ} in the amorphous region. It would also help to explain the f_{MQ} dependence on coupling strength which will be discussed later in this paper.

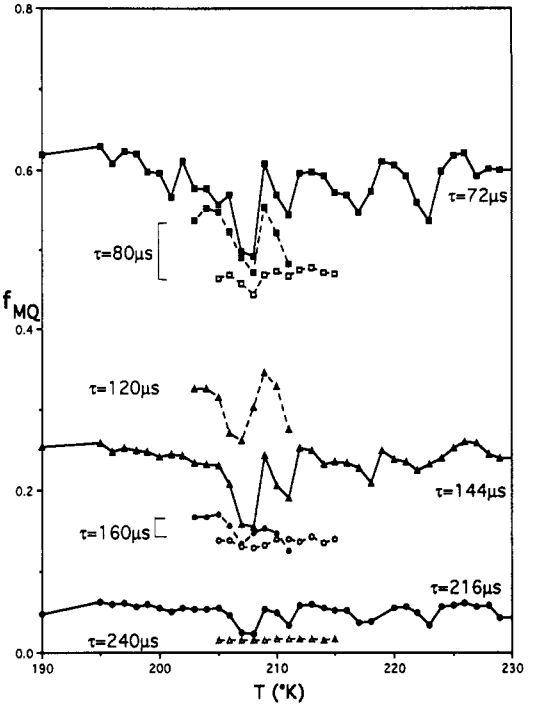

Figure 7. Fractional signal intensity, f_{MQ}, in as-polymerized PTFE from 190 to 230 K. The oscillations seen for the as-polymerized sample (solid symbols) are attributed to cyclic motion in the paracrystalline regions. Also shown are the results of separate experiments on both samples between 202 and 215 K. The data from the as-polymerized sample (solid symbols) confirm the reproducibility of the f_{MQ} measurement. The data for the melt-crystallized sample (open symbols) do not show the oscillations observed for the as-polymerized sample.

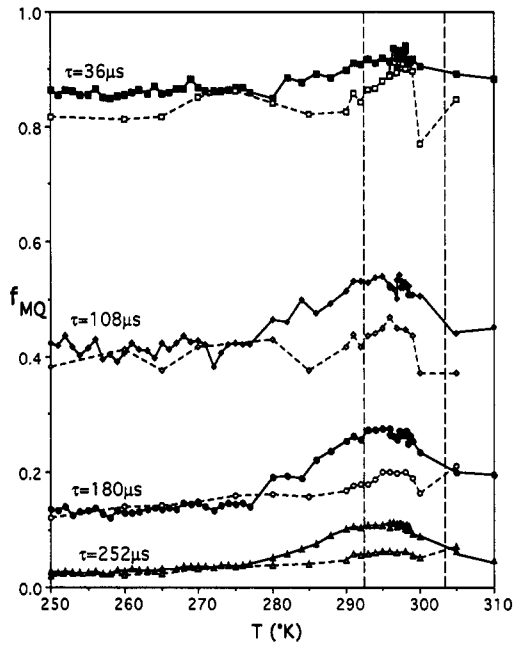

Figure 8. Fractional signal intensity, f_{MQ}, in 64% crystalline, melt-crystallized (open symbols) and as-polymerized (solid symbols) PTFE from 250 to 310 K. The f_{MQ} increase seen in both samples near the two crystalline transitions (vertical lines) is attributed to the slowing of MQ coherence growth upon the motional averaging of internuclear couplings, caused by high-frequency chain rotations in the crystalline regions. The rapid dropoff seen near the second transition is attributed to the chain slippage and random segment reorientation introduced at this temperature.

At about 150 K, in Figure 6, we see the f_{MQ} values for the melt-crystallized sample begin to decrease until they are below the values for the as-polymerized sample at 200 K. The as-polymerized sample, which lacks amorphous

regions, has a relative constant value of f_{MQ} over this same temperature range. This temperature range corresponds to the γ-relaxation seen in dielectric and mechanical relaxation data and the onset of segmental motion in the amorphous chains.[25] We attribute the overall drop in the measured f_{MQ} values of the melt-crystallized sample with temperature to motions associated with the γ-relaxation which interfere with the signal refocusing process as described earlier.

Figure 7 shows the f_{MQ} values obtained for the as-polymerized sample at three different preparation times for 195–250 K. The most obvious aspect of Figure 7 is the variation in f_{MQ} values that begins about 208 K and continues with decreasing amplitude toward higher temperatures. A viscoelastic anomaly associated with the motion of defects through the intermediate paracrystalline regions has previously been reported in as-polymerized samples over this same temperature range.[28] Also shown in Figure 7 are the results obtained by a repeat of the experiment several weeks later on both samples over a smaller temperature range under slightly different experimental conditions (2-μs pulse, 40-μs cycle, thermocouple recalibrated). The pattern of values in the data for the as-polymerized sample in this later experiment (dotted line, closed symbols) corresponds well with the original data in terms of its dependence on both temperature and τ. By contrast, the f_{MQ} values are relatively constant over this same temperature range for the melt-quenched PTFE (dotted line, open symbols). The lack of oscillations in the f_{MQ} data for the melt-crystallized sample is consistent with the absence of a viscoelastic anomaly in melt~quenched samples,[28] and this further makes it clear that the f_{MQ} oscillations and the viscoelastic anomaly in the as-polymerized sample are related to the same motional process.

At this point, we cannot rigorously explain the source of these f_{MQ} variations. We do not expect that the nature of the motion is changing much through this temperature range. What does change, however, is the relation of the motional frequency to the experimental time frame. It is possible to imagine motions in which the motional frequency is on the order of the evolution time τ but which will not cause an f_{MQ} decrease. More specifically, motion which is able to restore the nuclei involved in the MQ coherences to their original positions during the course of the experiment could possibly aid refocusing.

We must also consider the effect the motion might have on relaxational processes responsible for the f_{MQ} decrease observed even in static samples. The fact that the overall f_{MQ} intensity does not decrease over the temperature range seen in Figure 7 indicates that the motion does not involve the random internuclear vector variations which would be associated with chain slippage or orientational drift and would be expected to help destroy refocusing of the coherences. More work is needed to fully determine what information on the frequency and identity of the motion can be obtained from the data, and this will remain a goal in our future work.

Seen in Figure 8 are the f_{MQ} data for both samples from 250 to 310 K. For clarity, only four of the seven preparation cycle times are shown. The first thing we note in Figure 8 is a rise in the f_{MQ} values with increasing temperature between about 260 K and the first-order crystalline transitions at 292 and 303 K. The f_{MQ} increase is larger in the as-polymerized sample compared to the melt-crystallized sample due to the greater crystalline fraction in the as-polymerized sample. The rise in the f_{MQ} values corresponds to the decrease in the second moment due to motional narrowing, as seen in previous NMR studies.[19] The importance of this motional decoupling for the f_{MQ} values can be seen in Figure 9.

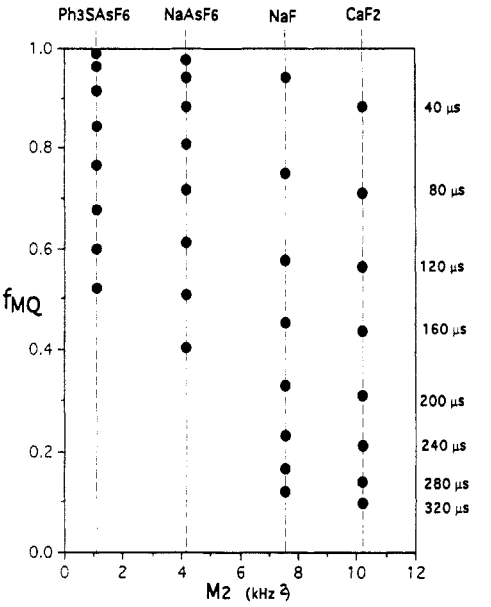

Figure 9. Fractional signal intensity, f_{MQ}, for several crystalline compounds, showing the f_{MQ} dependence on the average dipolar coupling strength (M_2) as calculated from published crystal structures.

Figure 9 shows the f_{MQ} values for four crystalline compounds as a function of the dipolar coupling strength within the crystal. The four crystals shown are sodium fluoride, calcium fluoride, and two hexafluoroarsenate salts. The dipolar couplings for the fluorides are assumed to be static, but the intramolecular couplings for the hexafluoroarsenate salts are averaged to zero on the NMR time scale by rapid isotropic motion of the AsF_6^- ions.[8] The τ-dependent decay of f_{MQ} intensity is clearly also dependent on the strength of the dipolar couplings and thus the rate of coherence buildup. This provides an explanation for the increase of temperature-dependent f_{MQ} values between 260 and 295 K in PTFE, since high-frequency chain rotations are known to average the dipolar couplings in this range.[19]

Near the second crystalline transition in Figure 8, we see a sudden dropoff in the f_{MQ} intensity values. This region corresponds to the onset of incoherent rotations and translational chain slippage in the crystalline chains as described earlier. We attribute the dropoff in f_{MQ} intensity seen near the second crystalline transition at 303 K to the destruction of the intermediate-range structural order, upon which the coherence growth and thus the signal refocusing depend.

A final observation is that f_{MQ} at a given τ gives nearly the same constant value over the ranges $110 < T < 190$ K and $250 < T < 270$ K in the as-polymerized sample (Figures 4, 6, and 8). In addition, this same f_{MQ} value for a given τ is observed in the melt-crystallized sample from 250 to 270 K (Figures 5 and 8). This indicates the dipolar field in these three regimes is similar and, furthermore, provides strong evidence for the reproducibility of the f_{MQ} measurement.

Conclusions

We have shown how MQ-NMR intensity data can be used to probe the effect of motion on the dipolar relationships among the spins of coherent spin clusters. Unlike other techniques, it is sensitive to the effects of motion on the intermediate-range structural order of the

material. Thus, a simple rotation, which preserves intermediate-range order, will have a different effect than a random translation, which will not preserve the intermediate-range order. Before we are able to draw any quantitative conclusions based on this experiment, we must address two issues. The first is to be able to rigorously treat the refocusing of the coherences under different kinds of motion. Although static MQ coherence growth can be described using density matrix calculations, they are prohibitive timewise for even small spin clusters ($N_e > 9$).[29] The second challenge is to understand the source of the f_{MQ} decrease with τ in motionally static samples and the effect motion might have on this process.

The trends in our data can qualitatively be explained in terms of what is already known about the motion in PTFE. The temperature-dependent f_{MQ} increase seen in Figure 8 between 270 and 300 K is readily explained by the high-frequency simple chain rotations which occur here. The temperature-dependent f_{MQ} decreases seen between 160 and 200 K in Figure 6 and between 295 and 310 K in Figure 8 can likewise be explained by random chain translations and reorientations which are present in the crystalline regions above 303 K and in the amorphous regions beginning about 160 K, respectively. In contrast, less is known about the paracrystalline defect motion beginning at 208 K, but our data seem to indicate that the motion preserves the intermediate-range structural order on the experimental time frame and that this motion only occurs in the as-polymerized sample. We also speculate that the relationship of the frequency of conformational conversion to the experimental time frame is responsible for the f_{MQ} oscillations seen in Figure 7.

Acknowledgment. The authors gratefully acknowledge the National Science Foundation, Grant No. CTS9057119. We would also like to thank Ted Treat and Paul Resnick at DuPont for the samples studied and Bruce Scruggs for valuable help.

References and Notes

(1) Yen, Y.; Pines, A. *J. Chem. Phys.* **1983**, *78*, 3579.
(2) Baum, J.; Gleason, K. K.; Pines, A.; Garroway, A. N.; Reimer, J. A. *Phys. Rev. Lett.* **1986**, *56*, 1377. Gleason, K. K.; Petrich, M. A.; Reimer, J. A. *Phys. Rev. B* **1987**, *36*, 3259.
(3) Petrich, M. A.; Gleason, K. K.; Reimer, J. A. *Phys. Rev. B* **1987**, *36*, 9722.
(4) Levy, D. H.; Gleason, K. K. *J. Phys. Chem.* **1992**, *96*, 1992.
(5) Ryoo, R.; Liu, S. B.; de Menorval, L. C.; Takegoshi, K.; Chmelka, B.; Trecoske, M.; Pines, A. *J. Phys. Chem.* **1987**, *91*, 6575. Chmelka, B.; Pearson, J. G.; Liu, S. B.; Ryoo, R.; de Menorval, L. C.; Pines, A. *J. Phys. Chem.* **1991**, *95*, 303.
(6) Wang, P. K.; Slichter, C. P.; Sinfelt, J. H. *Phys. Rev. Lett.* **1984**, *53*, 82.
(7) Scruggs, B. E.; Gleason, K. K. *J. Magn. Reson.* **1992**, *99*, 149.
(8) Scruggs, B. E.; Gleason, K. K. *Macromolecules* **1992**, *25* (7), 1864.
(9) Pines, A.; Rhim, W. K.; Waugh, J. S. *J. Magn. Reson.* **1972**, *6*, 457.
(10) Emid, S. *Physica* **1985**, *128B*, 79.
(11) Munowitz, M. *Mol. Phys.* **1990**, *71* (5), 959.
(12) Ernst, R. R.; Bodenhausen, G.; Wokaun, A. *Principles of Nuclear Magnetic Resonance in One and Two Dimensions*; Clarendon Press: Oxford, 1987: pp 534–5.
(13) Mehring, M. *Principles of High Resolution NMR in Solids*; Springer: Berlin, 1983; Chapter 3.
(14) Baum, J.; Pines, A. *J. Am. Chem. Soc.* **1986**, *108*, 7447.
(15) Baum, J.; Munowitz, M.; Garroway, A. N.; Pines, A. *J. Chem. Phys.* **1985**, *83* (5), 2015.
(16) Bunn, C. W.; Howells, E. R. *Nature* **1954**, *174*, 549.
(17) Clark, E. S.; Muus, I. T. *Z. Kristallogr., Kristallgeom., Kristallphys.* **1962**, *117*, 119.
(18) Lau, S. F.; Suzuki, H.; Wunderlich, B. *J. Polym. Sci., Polym. Phys. Ed.* **1984**, *22*, 379.
(19) Eby, R. K.; Sinnott, K. M. *J. Appl. Phys.* **1961**, *32* (9), 1765. Slichter, W. P. *J. Polym. Sci.* **1957**, *24*, 173. Smith, J. A. *Discuss. Faraday Soc.* **1955**, *19*, 207.
(20) Vega, A. J.; English, A. D. *Macromolecules* **1980**, *13*, 1635.
(21) McCall, D. W.; Douglass, D. C.; Falcone, D. R. *J. Phys. Chem.* **1967**, *71*, 998.
(22) Takenaga, M.; Obori, H.; Yamagata, K. *J. Polym. Sci., Polym. Lett. Ed.* **1985**, *23*, 45.
(23) Ohazwa, Y.; Wada, Y. *Jpn. J. Appl. Phys.* **1964**, *3* (8), 436.
(24) Krum, F.; Müller, F. *Kolloid Z.* **1959**, *164*, 81.
(25) McCrum, N. G.; Read, B. E.; Williams, G. *Anelastic and Dielectric Effects in Polymer Solids*; Wiley: New York, 1967.
(26) Wada, Y.; Hayakawa, R. *Progress in Polymer Science, Japan*; Okamura, S., Takayanagi, M., Eds.; Kodansha: Tokyo, 1972; Vol. 3.
(27) Starkweather, H.; Zoller, P.; Jones, G.; Vega, A. *J. Polym. Sci., Polym. Phys. Ed.* **1982**, *20*, 751.
(28) Takenaga, M.; Yamagata, K.; Kasai, A.; Ariyama, T. *J. Appl. Polym. Sci.* **1990**, *39*, 1689.
(29) Munowitz, M. *Mol. Phys.* **1990**, *71*, 959. Scruggs, B. E.; Gleason, K. K. *Chem. Phys.* **1992**, *166*, 367.